The results of analyzing the railroad track as a lossy waveguide illustrate the usefulness of the numerical method developed. In addition, the proposal to use the track as a waveguide was shown to warrant further investigation as a viable alternative for collision avoidance or headway control in future rapid-transit systems.

References

[1] W. M. Elsasser, "Attenuation in a dielectric circular rod," *J. Appl. Phys.*, vol. 20, pp. 1193–1196, Dec. 1947.
[2] A. Sommerfield, *Electrodynamics*. New York: Academic, 1964, pp. 177–192.
[3] Z. J. Czendes and P. Silvester, "Numerical solutions of dielectric loaded waveguides: I—Finite element analysis," *IEEE Trans. Microwave Theory Tech.*, vol. MTT-18, pp. 1124–1131, Dec. 1970.
[4] S. Ahmed, "Finite-element method for waveguide problems," *Electron. Lett.*, vol. 4, pp. 387–389, 1968.
[5] P. Daly, "Hybrid mode analysis of microstrip by finite element methods," *IEEE Trans. Microwave Theory Tech.*, vol. MTT-19, pp. 19–25, Jan. 1971.
[6] B. H. McDonald and A. Wexler, "Finite-element solution of unbounded field problems," *IEEE Trans. Microwave Theory Tech.*, vol. MTT-20, pp. 841–847, Dec. 1972.
[7] S. Ahmed and P. Daly, "Waveguide solutions by the finite element method," *Radio Electron. Eng.*, vol. 38, p. 217, Oct. 1969.
[8] ——, "Finite element methods for inhomogeneous waveguides," *Proc. IEE*, vol. 116, p. 1661, Oct. 1969.
[9] P. L. Arlett *et al.*, "Application of finite elements to the solution of Helmholtz's equation," *Proc. IEE*, vol. 115, p. 1962, Dec. 1968.
[10] P. Daly, "Finite elements for field problems in cylindrical coordinates," *Int. J. Numer. Methods Eng.*, vol. 6, pp. 167–168, 1973.
[11] R. E. Collins, *Field Theory of Guided Waves*. New York: McGraw-Hill, 1960, p. 454.
[12] B. A. Finlayson, *Methods of Weighted Residuals and Variational Principles with Application in Fluid Mechanics, Heat and Mass Transfer*. New York: Academic, 1972, pp. 7–12, 299–232.
[13] A. D. McAulay, "Detection of track guided ground vehicles using the track as an electromagnetic waveguide," Ph.D. Thesis, Carnegie-Mellon Univ., 1974.
[14] ——, "The finite element solution of dissipative electromagnetic surface waveguides," *Int. J. Numer. Methods Eng.*, vol. 11, pp. 11–25, 1977.
[15] ——, "Track guided radar for rapid transit systems," *AIAA J. Aicraft*, vol. 12, pp. 676–681, Sept. 1975.
[16] ——, "Progress in signaling for track guided systems," *Transportation Eng. J. ASCE*, vol. 101, no. TE4, pp. 621–637, Nov. 1975.
[17] O. C. Zienkiewitz and Y. K. Cheung, *The Finite Element Method in Structural and Continuum Mechanics*. New York: McGraw-Hill, 1970.
[18] J. T. Oden, *Finite Element of Non-Linear Continua*. New York: McGraw-Hill, 1972.
[19] S. G. Miklin and K. L. Smolitsky, *Approximate Methods for the Solution of Differential and Integral Equations*. New York: Elsevier, 1967, ch. 3.
[20] D. J. Richards and A. Wexler, "Finite element solutions within curved boundaries," *IEEE Trans. Microwave Theory Tech.*, vol. MTT-20, p. 650, Oct. 1972.
[21] P. Silvester, "High order polynomial triangular finite elements for potential problems," *Int. J. Eng. Sci.*, vol. 7, p. 849, Aug. 1969.
[22] P. Daly, "Finite element coupling matrices," *Electron. Lett.*, vol. 5, p. 613, Nov. 1969.
[23] C. B Moler and G. W. Stewart, "An algorithm for the generalized matrix eigenvalue problem $Ax = \lambda Bx$," CS-232-71, Stanford Univ.
[24] G. Goubau, "Surface waves and their application to transmission lines," *J. Appl. Phys.*, vol. 21, pp. 1119–1128, Nov. 1950.
[25] H. M. Barlow and J. Brown, *Radio Surface Waves*. Oxford: Oxford University Press, 1962.
[26] *Reference Data for Radio Engineers*, ITT, 5th ed., 1969.
[27] A. S. Hu, "Transmission properties of waveguide communication systems," *Proc. IEEE*, vol. 61, pp. 556–561, May 1973.
[28] H. R. Reed and C. M. Russell, *Ultra-High Frequency Propagation*. New York: Wiley, 1953, p. 24.

Aperture Coupling Between Microstrip and Resonant Cavities

DAVID S. JAMES, MEMBER, IEEE, GUY R. PAINCHAUD, MEMBER, IEEE, AND WOLFGANG J. R. HOEFER, MEMBER, IEEE

Abstract—**This paper presents a simple analysis for the coupling between microstrip and a cavity through an aperture located in the substrate ground plane. The analysis is based on Wheeler's equivalent-energy concept for small-hole coupling and an approximate parallel-plate waveguide model for the microstrip. The theory appears adequate for most design purposes, and has been used successfully in the design of stabilizing cavities for experimental 12-GHz low-noise FET oscillators.**

I. Introduction

THE PURPOSE of this paper is to present an analysis and experimental data on the performance of a novel microstrip-to-cavity transition, so that high Q cavities can be made compatible with existing MIC techniques. Previous authors [1]–[5] have described empirically designed microstrip and stripline-to-waveguide transitions; however, with the exception of [4], none of these papers describe coupling to a resonant cavity.

The transition studied is shown in Fig. 1. The ground plane of the microstrip substrate forms one of the cavity end plates. In particular, we have investigated coupling to cylindrical cavities resonating in the TE_{01n} mode. Coupling is by means of an aperture located in the ground plane at the point of maximum radial H-field in the cavity. The microstrip line terminates in an open circuit $3\lambda_g/4$ beyond the aperture. This length of line maximizes the coupling through the aperture [6]–[8]. This configuration is quite practical, as the cavity can be machined into the substrate holder.

Unfilled cavities can readily yield values of unloaded $Q(Q_0)$ of at least 25 000. This value is much greater than that of both planar resonators ($Q_0 < 500$) [9] and "open"

Manuscript received December 10, 1975; revised August 9, 1976.

D. S. James was with the Department of Communications, Communications Research Centre, Ottawa, Ont., Canada. He is now with the Ferranti Solid State Microwave Group, Manchester, U.K.

G. R. Painchaud was with the Department of Electrical Engineering, University of Ottawa, Ottawa, Ont., Canada. He is now with the Department of Communications, Communications Research Centre, Ottawa, Ont., Canada.

W. J. R. Hoefer is with the Space Division, AEG-Telefunken, Backnang, Germany, on leave from the Department of Electrical Engineering, University of Ottawa, Ottawa, Ont., Canada.

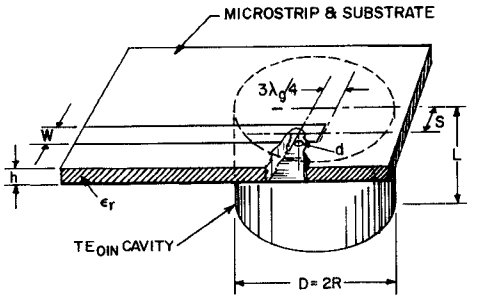

Fig. 1. Coupling arrangement between microstrip and a TE_{01n} cavity. Coupling is by means of an aperture of diameter d located in the substrate ground plane.

dielectric resonators ($Q_0 < 5000$) [10] used in current MIC designs. Furthermore, the coupling coefficient is easily calculated for our coupling arrangement; this is not so in the case of an open dielectric resonator coupled to a microstrip line [10]. Suitable choice of a temperature-stable cavity material [7], [8] can simultaneously provide long-term frequency stability unattainable from other forms of resonators used for MIC's.

The technique has been successfully applied to the design of stabilizing cavities for experimental low-noise 12-GHz FET oscillators. [7], [8].

II. Analysis of the Transition

A rigorous analysis of the transition shown in Fig. 1 is quite formidable, as the microstrip is an inhomogeneous structure, and no closed-form solution is available. Since in most applications cavities are undercritically coupled to conserve a high Q factor, Wheeler's equivalent energy concept [11] for calculating the coupling through small apertures is employed. The assumption is made that the field is uniform over the aperture. The analysis yields a simple expression which we have experimentally verified and found useful for design purposes.

Wheeler has shown that the coupling between a waveguide and a resonant cavity can be evaluated by considering two symmetrical coupling problems. a) The coupling between two waveguides due to a small aperture of normalized reactance x in a common wall. In our case, the waveguides consist of two microstrip lines, each terminated at one end by an open-circuit stub an odd number of quarter-wavelengths from the aperture. b) The coupling between two identical cavities by the same aperture, characterized by a coupling factor k.

The loading power factor p is then given as [11]

$$p = \frac{1}{Q_{ext}} = kx, \qquad \text{with error } 0(p). \tag{1}$$

In the following text, Q_{ext} is calculated by employing the equivalent-energy concept and a simplified parallel-plate waveguide model for the microstrip. The ground plane is assumed to have negligible thickness.

A. Aperture Coupling Between Two Identical TE_{01n} Cavities

The cavity used is cylindrical, with a radius R and length L resonating in a TE_{01n} mode at frequency f_0 (see Fig. 1). The TE_{01n} modes are used, as they yield the highest Q for a given volume [12], and good electrical contact is not necessary between the cavity walls and end plates.

As the E-field is zero everywhere near the cavity walls for the TE_{01n} modes, only magnetic coupling can be used. The coupling factor k_m for such coupling between two identical resonant cavities is [11]

$$k_m = \frac{1}{4}\frac{V_{mc}}{V_m}. \tag{2}$$

Here V_{mc} is the effective volume of the coupling aperture as defined by Wheeler and V_m is the effective volume of the cavity. The effective volume is that volume which, when uniformly filled with the field existing at the position of the aperture, stores the same amount of energy as the actual cavity.

The cavity effective volume then satisfies the following relation:

$$\tfrac{1}{2}\mu H_c^2 V_m = \tfrac{1}{2}\mu \int_{\text{cavity}} H^2\, dV. \tag{3}$$

The quantity H_c is the field that is tangential to the cavity wall at the location of, but in the absence of, the aperture. The location of the aperture (distant S from center in Fig. 1) is chosen to coincide with the position of maximum radial H-field. This choice gives the strongest coupling for a given aperture. From [12], the tangential H-field at the ends of the cavity for the TE_{01n} modes is

$$H_r = -\frac{k_3}{k_0} J_1(k_1 r) \tag{4}$$

where $k_0^2 = \omega^2\mu\varepsilon$, $k_1 = r_{11}/R$, $k_3 = n\pi/L$, and r_{11} is the first root of $J_1(\xi) = 0$.

The value of S satisfies the following:

$$\frac{\partial}{\partial_r}\left(\frac{-k_3}{k_0} J_1(k_1 r)\right)\bigg|_{r=S} = 0. \tag{5}$$

Thence $S = 0.481R$ and the value of H_c is found by substituting $r = S$ into (4).

Taking the expressions for H from [12], the effective volume is obtained using (3):

$$V_m = \frac{\int_{\text{cavity}} H^2\, dV}{H_c^2} = \frac{\dfrac{\pi L R^2}{2}\left[J_0(k_1 R)\right]^2}{\left[\dfrac{-k_3}{k_0} J_1(k_1 S)\right]^2}. \tag{6}$$

For a circular aperture of diameter d, the value of V_{mc} is [11]

$$V_{mc} = \tfrac{2}{3}d^3. \tag{7}$$

The value of k_m is obtained from (2), (6), and (7):

$$k_m = \tfrac{1}{4}\cdot\tfrac{2}{3}d^3 \frac{\left[\dfrac{-k_3}{k_0} J_1(k_1 S)\right]^2}{\dfrac{\pi L R^2}{2}\left[J_0(k_1 R)\right]^2}. \tag{8}$$

B. Aperture Coupling Between Two Identical Microstrips

An expression will here be derived for the normalized reactance x of a small aperture coupling two microstrips together that share a common ground plane, as shown in

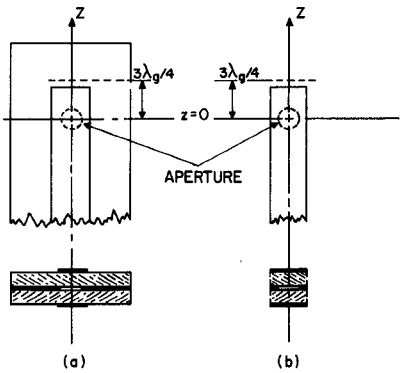

Fig. 2. (a) Aperture coupling between two identical microstrips. (b) Aperture coupling between two identical parallel-plate waveguides with magnetic side walls.

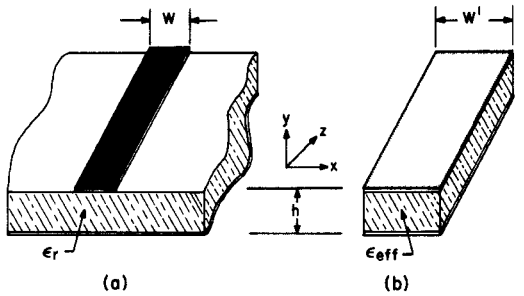

Fig. 3. (a) Cross section of a microstrip transmission line. (b) Equivalent parallel-plate waveguide with magnetic side walls.

Fig. 2(a). For this purpose, the microstrip coupling configuration of Fig. 2(a) is modeled by that shown in Fig. 2(b), which illustrates the coupling between two parallel-plate guides due to an aperture in a common wall.

The equivalence between microstrip and a parallel-plate waveguide with magnetic side walls was used for discontinuity calculations by Leighton and Milnes [13], based on earlier work by Oliner [14] for stripline. As shown in Fig. 3, the parallel-plate guide is assumed to be uniformly filled with dielectric of relative value ε_{eff}; this value includes the effect of dispersion. The width W' and guide wavelength λ_g of the parallel-plate guide are

$$W' = \frac{h}{Z_0}\frac{\eta_0}{\sqrt{\varepsilon_{\text{eff}}}} \tag{9}$$

$$\lambda_g = \frac{\lambda_0}{\sqrt{\varepsilon_{\text{eff}}}} \tag{10}$$

where λ_0 is the free-space wavelength and $\eta_0 = 377\ \Omega$.

The field components for the TEM mode in the parallel-plate waveguide model are

$$E_y = \left(\frac{\eta_0}{\sqrt{\varepsilon_{\text{eff}}}}\right) H_0 \exp\left(j\frac{2\pi}{\lambda_g} z\right) \tag{11}$$

$$H_x = H_0 \exp\left(j\frac{2\pi}{\lambda_g} z\right). \tag{12}$$

The normalized reactance of a small aperture is given in terms of the transmission coefficient T [15] as

$$x = \frac{T}{2j}. \tag{13}$$

From [15], the transmission coefficient T through an aperture as shown in Fig. 2(b) is

$$T = \frac{2\pi j}{S_0\lambda_g}\left(M_1 H_{0l} H_l + M_2 H_{0m} H_m + P E_{0n} E_n\right) \tag{14}$$

where the variables are as defined in [15].

In our particular case [Fig. 2(b)], the last two terms of (14) are equal to zero, and $H_{0l}H_l = 2H_0^2$. For the circular aperture used here the value of M_1 is well known [15]:

$$M_1 = \tfrac{1}{6}d^3. \tag{15}$$

Also, the normalizing factor S_0 is found to be [15]

$$S_0 = H_0^2 h W'. \tag{16}$$

Combining equations (13)–(16), the value of the normalized reactance is then found to be

$$x = \frac{\pi d^3}{3W'h\lambda_g}. \tag{17}$$

C. Aperture Coupling Between Microstrip and a TE_{01n} Cavity

The external Q of the cavity due to the loading of the microstrip is finally obtained from (1), (8)–(10), and (17) as (MKS units)

$$Q_{\text{ext}} = 5.423 \times 10^{-6}\frac{f_0 L^3 D^2 h^2}{n^2 Z_0 \varepsilon_{\text{eff}} d^6}. \tag{18}$$

The coupling coefficient is then given as

$$\beta = \frac{Q_0}{Q_{\text{ext}}}. \tag{19}$$

The approximation that the H-field is constant over the aperture deteriorates as the ε_r of the substrate increases and λ_g decreases. To account for this, a first-order correction was applied to the expression for the external Q by using the average value of the H-field over the aperture in the calculation of (1). This normalized average value is

$$\frac{H_{\text{avg}}}{H_{\text{max}}} = \frac{\int_{\text{aperture}} \cos\left(\frac{\pi d}{\lambda_g} z\right) dA}{\text{aperture area}} = \frac{2\lambda_g}{\pi d} J_1\left(\frac{\pi d}{\lambda_g}\right). \tag{20}$$

The corrected value for Q_{ext} is obtained by dividing (18) by a correction factor q. The latter is obtained from (20) as

$$q = \left(\frac{2J_1(\theta)}{\theta}\right)^2, \qquad \theta = \frac{df_0\sqrt{\varepsilon_{\text{eff}}}}{9.55 \times 10^7}. \tag{21}$$

A similar correction factor could be applied for the transverse variation in the H-field. However, the field variation in this direction is not as rapid as that in the direction of propagation and we believe that it is sufficient to include a correction for the first case only. From ground-plane current-density distributions obtained by finite-difference computations [16], we estimate the correction for the H-field variation in the x-direction is less than 10 percent, even for the largest anticipated apertures.

In a practical design problem, the microstrip parameters would normally be chosen first. The aperture diameter required to yield a particular β would then be determined from (18) and (19). It should be noted, however, that for

TABLE I
PARAMETERS FOR *S*-BAND MICROSTRIP COUPLING CIRCUITS ON OVERSIZED REXOLITE AND STYCAST SUBSTRATES

Substrate	ε_r	ε_{eff}	Z_0 (Ω)	W(in)	h(in)	S(in)
Rexolite	2.6	2.27	50	0.541	0.200	1.354
Stycast	10.0	9.45	23	0.626	0.200	1.354

relatively high values of Z_0, (18) can lead to values for the aperture diameter d much greater than the microstrip linewidth W. If this occurs, a wider line (lower Z_0) should then be chosen. It is often convenient to use other shapes of aperture. For example, compared to a circular aperture of diameter d, a rectangular one of length $d/2$ and width d yields a coupling coefficient only 11 percent less for small apertures [11]. The corresponding correction factor q is now $(\sin \theta/\theta)^2$ for large apertures.

III. EXPERIMENTAL VERIFICATION OF THE TRANSITION

The expression for the external Q derived in the previous section was experimentally verified using a transmission cavity. The measurements were made at *S*-band in order to reduce the effects of dimensional tolerances.

A cavity was designed to resonate in the TE_{012} mode at 3.333 GHz. The dimensions were obtained from [12] and are $D = 5.628$ in and $L = 5.517$ in.

The cavity was machined from brass and silver plated. An end plate was also made with a small coupling loop that terminated into a 3-mm coaxial connector. The loop was oriented to couple to the maximum H-field of the TE_{012} mode. The theoretical Q_0 of the plated cavity is approximately 64 000. A lossy mode supressor in the form of a gasket was machined from Synthane and served to effectively suppress the companion TM_{112} mode.

Two microstrip circuits were made, one on a Rexolite ($\varepsilon_r = 2.6$) substrate and the other on Stycast ($\varepsilon_r = 10.0$). At first it seemed desirable to make the characteristic impedance Z_0 equal to 50 Ω on both substrates; however, for the Stycast substrate, this gives a linewidth that is smaller than the aperture diameter at critical coupling (see Section II-C). A lower Z_0 (wider line) was consequently used; $Z_0 = 23$ Ω was found convenient. The microstrip parameters were calculated with a computer program based on Getsinger's model [17] (which we have found accounts well for dispersion) and are given in Table I. The physical length of the $3\lambda_g/4$ stub includes a correction for the end-effect [18]. Anomalous behavior can often be observed when the stub is $\lambda_g/4$ rather than $3\lambda_g/4$, $5\lambda_g/4$, etc. This is thought to be due to the interaction between the stub end and the coupling region, and leads to measured values for β lower than expected. The Stycast substrate and *S*-band cavity are shown in Fig. 4. The mode suppressor is located between the bottom plate and the cavity walls.

A. Experimental Results

The cavity was measured under transmission; this reduces the effects of launcher discontinuities and simplifies the Q measurement. The aperture in the microstrip ground plane formed the input coupling port and the small coupling loop in the end plate was the output (detector) port. For measurement convenience, the coupling loop in the end plate was initially adjusted to make its coupling coefficient approximately unity. The aperture diameter was then increased in steps and the insertion loss and 3-dB bandwidth, Δf, were measured each time [19]. The results are given in Fig. 5 for both substrates.

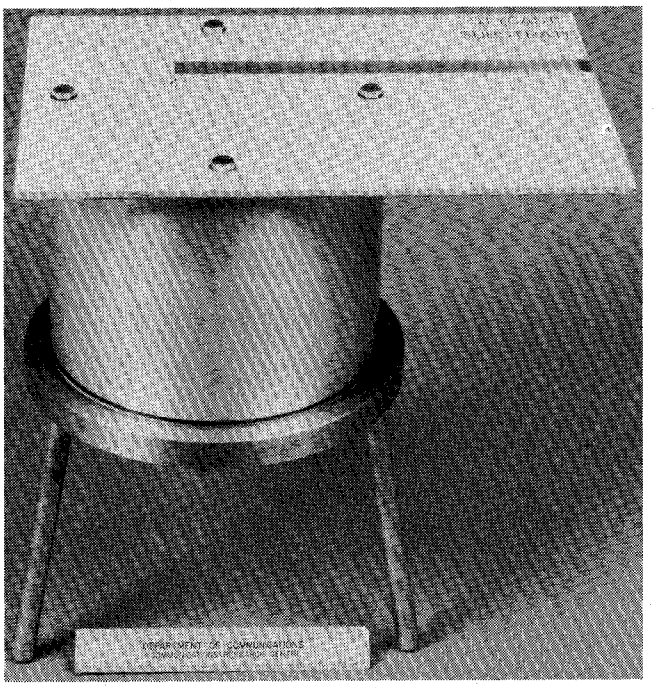

Fig. 4. The *S*-band cavity with the Stycast substrate in place. The 3-mm connector for the output coupling loop is mounted in the bottom plate (not visible).

It can be seen from Fig. 5 that for small values of β (i.e., small aperture diameters), the insertion loss is more sensitive to a change in β; whereas, for values of β about critical coupling or higher the bandwidth measurement is more sensitive. The coupling coefficient can be measured quite accurately over several decades using both sets of measurements.

Fig. 6 compares theoretical and measured values for the coupling coefficient β. The experimental values were obtained using the equivalent circuit and (27) and (28) presented in the Appendix. The theoretical curves represent values of β obtained from expressions (18) and (19) with and without the correction factor (21).

As a consequence of the simple cutting method used to enlarge the aperture diameter, the circumference usually

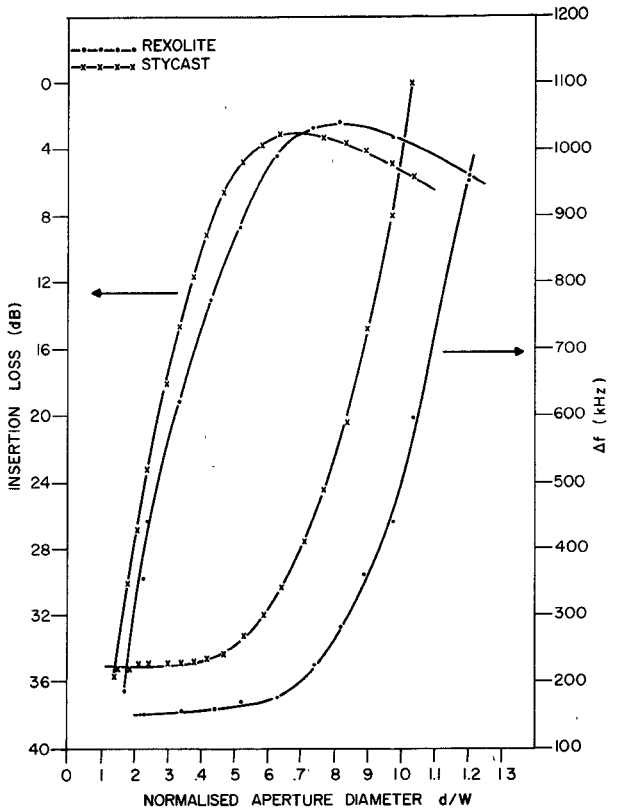

Fig. 5. Measured insertion loss and bandwidth Δf as a function of the normalized aperture diameter for coupling with Rexolite and Stycast substrates.

had a ripple of a few mils. Error bars on Fig. 6 show the change in β due to an estimated worst case peak-to-peak error of 0.010-in in the aperture diameter.

At critical coupling, the aperture diameter is $0.19\lambda_g$ for the Rexolite substrate and $0.38\lambda_g$ for the Stycast substrate. This explains why the measured values of β for the Stycast substrate seem to depart more from the simple theory than do those for the Rexolite substrate for large apertures.

We consider that the corrected expression is adequate for most design purposes.

IV. Applications

This section describes some further implementation of the coupling structure at 12 GHz which has successfully been incorporated in a stabilized FET oscillator.

A silver-plated cavity was designed to resonate at 12 GHz in the TE_{012} mode, and three different microstrip circuits were fabricated to fit on top of the cavity. The physical arrangement is depicted in Fig. 7.

The circuits were photoetched onto Ti:W–Au sputter-coated 2 × 2 × 0.025-in alumina substrates. Each circuit had two identical microstrip coupling ports with the cavity. For the reasons given in Section II-C, relatively wide lines ($Z_0 < 50\ \Omega$) were used for the transitions. Suitable tapers were included between the 50-Ω lines and the wider sections. The mode suppressor used in this case consisted of a discontinuous circular slot etched into the substrate ground plane, as shown in Fig. 8. The arrangement of the slot is

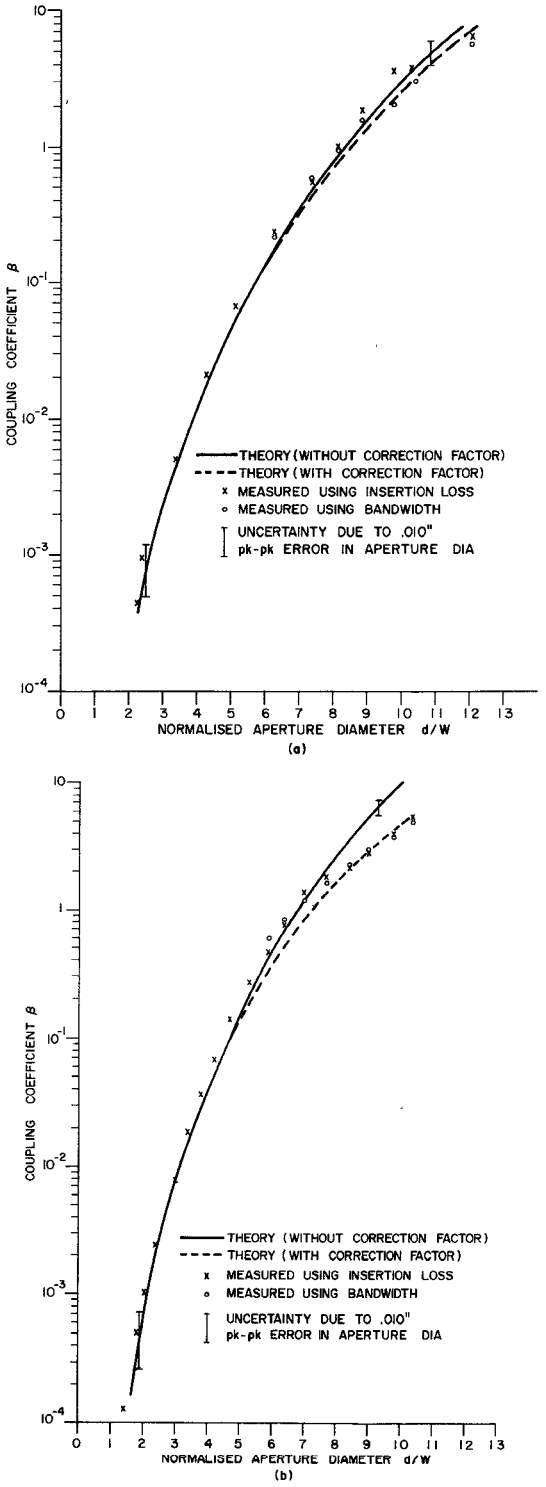

Fig. 6. Comparison of theoretical and measured values of the coupling coefficient β using (a) the Rexolite substrate and (b) the Stycast substrate.

such as to suppress modes other than those of type TE_{01n}; the slot is suitably interrupted in order not to perturb the two microstrip lines. It can be seen from Table II that agreement between theory and experiment is again quite good.

The previously mentioned cavity was successfully employed in an experimental phase-shift oscillator using a FET amplifier module; this same transmission cavity was

TABLE II
DATA AND PARAMETERS FOR 3 DIFFERENT 12-GHz MICROSTRIP CIRCUITS ON h = 0.025-IN ALUMINA SUBSTRATES, ε_r = 10

Circuit	Aperture Diameter (mils)	Zo (Ω)	Insertion Loss (dB)	Q_L	β-measured	Q_o	β-theory, without correction	β-theory, with correction
MIC-026	34.4	35	37.1	2.85×10^4	7.0×10^{-3}	2.89×10^4	7.1×10^{-3}	---
MIC-033	67.5	25	9.0	1.87×10^4	0.28	2.90×10^4	0.29	0.27
MIC-034	68.8	25	8.4	1.81×10^4	0.30	2.92×10^4	0.32	0.29

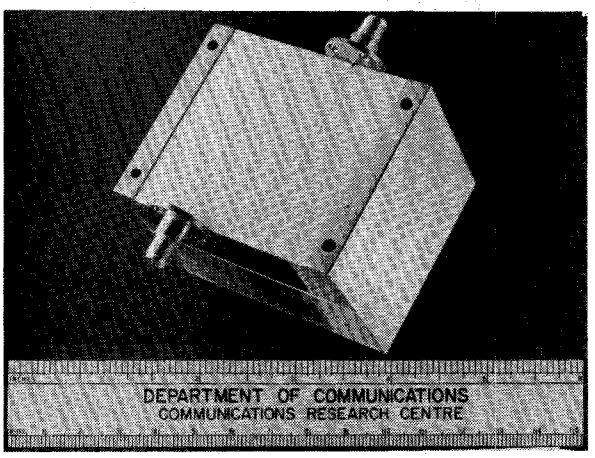

Fig. 7. Microstrip coupling to a TE_{012} cavity at 12 GHz (D = 1.667 in, L = 1.416 in). The cavity is machined into the substrate holder. Substrate ε_r = 10.

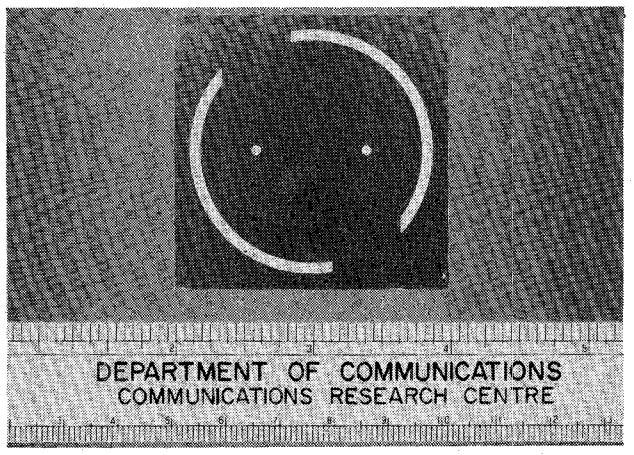

Fig. 8. Microstrip ground plane of the circuit shown in Fig. 7 illustrating the two coupling apertures and mode-suppressing slot.

also used to stabilize a one-port FET oscillator [7], [8]. The FM noise characteristics of these oscillators were comparable to that of a crystal-oscillator/multiplier source. Both types provided sufficient power for most LO applications.

V. CONCLUSION

An expression has been developed for the coupling coefficient of a TE_{01n} cavity coupled to a microstrip by means of an aperture in the microstrip ground plane. The theory was experimentally verified and found adequate for design purposes.

The configuration has been employed in the design of cavity stabilized FET oscillators.

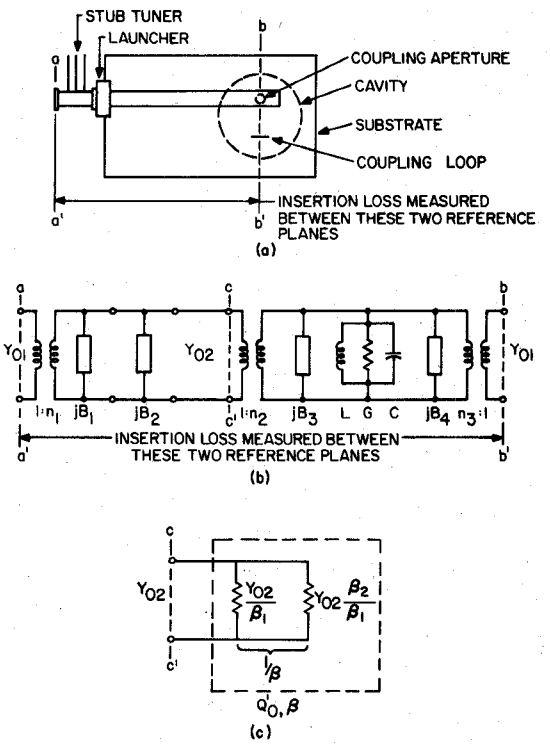

Fig. 9. (a) Schematic of the *S*-band cavity and associated coupling structures. (b) Equivalent circuit valid about the resonant frequency of the TE_{012} mode. (c) Simplified equivalent circuit viewed from c–c' with the terminated detector port (b–b') transformed into the cavity.

APPENDIX
CHARACTERIZATION OF THE *S*-BAND CAVITY

The equivalent circuit used to interpret the measurements and the physical structure it represents are shown in Fig. 9. This equivalent circuit represents the coupled cavity about the resonant frequency of the TE_{012} mode. The symbols used are defined as:

Y_{01}, Y_{02}	the characteristic admittances of the measurement setup and microstrip line;
n_1, jB_1	the transformer and susceptance representing the tuner;
jB_2	the discontinuity susceptance of the coaxial-to-microstrip transition;
n_2, jB_3, n_3, jB_4	these parameters characterize the aperture and the output coupling loop;
L, C, G	the parallel-tuned circuit represents the TE_{012} resonance.

The tuner was adjusted to match the admittance seen at the microstrip transition to that of the system. The shunt

susceptances jB_3 and jB_4 shift the resonant frequency slightly. As the resultant frequency shift is small (less than 600 kHz) and does not affect the measurements, these susceptances are neglected.

The input and output coupling coefficients as defined in [15] are

$$\beta_1 = \frac{Y_{02}}{n_2{}^2 G} \qquad \beta_2 = \frac{Y_{01}}{n_3{}^2 G}. \tag{22}$$

In order to evaluate the coupling between the microstrip and the cavity, the latter is considered as a one-port structure at reference planes c–c' with the detector port b–b' transformed into the cavity. The unloaded Q and coupling coefficient for the cavity as a one port at c–c' are

$$Q_0{}' = \frac{\omega C}{G(\beta_2 + 1)} = \frac{Q_0}{\beta_2 + 1} \tag{23}$$

$$\beta = \frac{Y_{02}}{n_2{}^2 G(\beta_2 + 1)} = \frac{\beta_1}{\beta_2 + 1}. \tag{24}$$

The insertion loss [IL in (25)] measured between a–a' and b–b' in Fig. 9(b) is equivalent to that measured between c–c' and the transformed detector impedance $Y_{02}(\beta_2/\beta_1)$ in Fig. 9(c) and can be expressed as

$$\mathrm{IL} = \frac{4\beta}{(\beta + 1)^2} \frac{\beta_2}{(\beta_2 + 1)}. \tag{25}$$

The minimum insertion loss occurs when port c–c' is critically coupled to the microstrip ($\beta = 1$).

The ratio r between the insertion loss and the minimum insertion loss is

$$r = \frac{4\beta}{(\beta + 1)^2}. \tag{26}$$

The value of β obtained from the relative insertion loss is then

$$\beta = \left(\frac{2}{r} - 1\right) \pm \sqrt{\left(\frac{2}{r} - 1\right)^2 - 1}. \tag{27}$$

From a measurement of the loaded Q,Q_L,β is independently obtained as

$$\beta = \frac{Q_0{}'}{Q_L} - 1, \qquad Q_L = f_0/\Delta f. \tag{28}$$

Acknowledgment

The authors wish to thank E. Minkus for considerable technical assistance.

References

[1] M. V. Schneider, B. Glance, and W. F. Bodtmann, "Microwave and millimeter wave hybrid integrated circuits for radio systems," *Bell Syst. Tech. J.*, vol. 48, pp. 1714–1717, July–Aug. 1969.
[2] R. H. Kneu, "A new type of waveguide-to-stripline transition," *IEEE Trans. Microwave Theory Tech.*, vol. MTT-16, pp. 192–194, Mar. 1968.
[3] B. Glance and R. Trambarulo, "A waveguide to suspended stripline transition," *IEEE Trans. Microwave Theory Tech.*, vol. MTT-21, pp. 117–118, Feb. 1973.
[4] B. B. Van Iperen, "Design and construction of an inexpensive 20 GHz stabilized IMPATT oscillator in microstrip technique," in *Proc. European Microwave Conf.*, Hamburg, Sept. 1975, pp. 171–175.
[5] J. H. C. van Heuven, "A new integrated waveguide-microstrip transition," in *Proc. European Microwave Conf.*, Montreux, Sept. 1974, pp. 541–545.
[6] W. J. R. Hoefer and D. S. James, "Microstrip to waveguide coupling through holes," in *Proc. 5th Colloq. Microwave Communication*, Budapest, June 1974, pp. 221–231.
[7] G. R. Painchaud, M.A.Sc. Thesis, Dept. Elec. Eng., Ottawa Univ., Ottawa, Ont., Canada, 1975.
[8] D. S. James, G. R. Painchaud, E. Minkus, and W. J. R. Hoefer, "Stabilized 12 GHz MIC oscillators using GaAs FET's," in *Proc. European Microwave Conf.*, Hamburg, Sept. 1975, pp. 296–300.
[9] E. Belohoubek and E. Denlinger, "Loss considerations for microstrip resonators," *IEEE Trans. Microwave Theory Tech.*, vol. MTT-23, pp. 522–526, June 1975.
[10] W. R. Day, Jr., "Dielectric resonators as microstrip-circuit elements," *IEEE Trans. Microwave Theory Tech.*, vol. MTT-18, pp. 1175–1176, Dec. 1970.
[11] H. Wheeler, "Coupling holes between resonant cavities or waveguides evaluation in terms of volume ratios," *IEEE Trans. Microwave Theory Tech.*, vol. MTT-12, pp. 231–244, Mar. 1964.
[12] I. G. Nilson, C. W. Schramm, and J. P. Kinzer, "High Q resonant cavities for microwave testing," *Bell Syst. Tech. J.*, pp. 408–433, July 1946.
[13] W. H. Leighton and A. G. Milnes, "Junction reactance and dimensional tolerance effects on X-band 3 dB directional couplers," *IEEE Trans. Microwave Theory Tech.*, vol. MTT-19, pp. 818–824, Oct. 1971.
[14] A. A. Oliner, "Equivalent circuits for discontinuities in balanced strip transmission line," *IRE Trans. Microwave Theory Tech.*, vol. MTT-3, pp. 134–143, Mar. 1955.
[15] C. G. Montgomery, R. H. Dicke, and E. M. Purcell, *Principles of Microwave Circuits*. New York and Dover, 1965, ch. 6, pp. 176–179 ch. 7, pp. 228–230.
[16] Interim report on P.O. Contract 515900, Dept. Elec. Eng., University College of North Wales, Bangor, U.K., Apr. 1969.
[17] W. J. Getsinger, "Microstrip dispersion model," *IEEE Trans. Microwave Theory Tech.*, vol. MTT-21, pp. 34–39, Jan. 1973.
[18] D. S. James and S. H. Tse, "Microstrip end effects," *Electron. Lett.*, vol. 8, pp. 46–47, Jan. 1972.
[19] W. J. R. Hoefer and G. R. Painchaud, "Frequency markers providing resolution of 1 kHz for swept microwave measurements," *Electron. Lett.*, vol. 10, pp. 123–124, Apr. 1974.